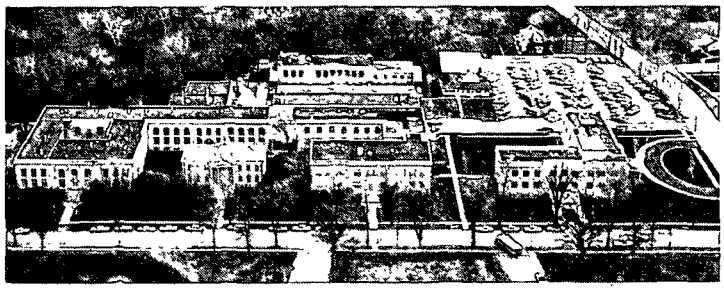

THE INSTITUTE OF PAPER CHEMISTRY, APPLETON, WISCONSIN

IPC TECHNICAL PAPER SERIES
NUMBER 218

SIMULATING THE DEVELOPMENT OF PULP AND PAPER PROPERTIES IN MECHANICAL PULPING SYSTEMS

GARY JONES

JANUARY, 1987

Simulating the Development of Pulp and Paper Properties in Mechanical Pulping Systems

Gary Jones

This manuscript is based on results of IPC dues funded research and is to be presented at a CPPA meeting in Montreal, Canada on January 28, 1987

SIMULATING THE DEVELOPMENT OF PULP AND PAPER PROPERTIES IN MECHANICAL PULPING SYSTEMS

GARY L. JONES
ENGINEERING DIVISION

THE INSTITUTE OF PAPER CHEMISTRY
APPLETON, WISCONSIN 54912

ABSTRACT

Process simulation, property modeling and optimization techniques have been combined in MAPPS (Modular Analysis of Pulp and Paper Systems) to predict optimum performance and quality of pulp and handsheet for high yield pulping systems. The structure is in place to simulate property development in kraft and sulfite pulping by the addition of the appropriate property models.

The technique involves the addition of a new set of fundamental variables called performance attributes or PAT's, which provide the link between the material and energy flows in the process and the predictive property models. In addition to property models, PAT models are used to predict the effect of refining, screening, cleaning, mixing and bleaching on the PAT's.

An optimization routine coupled with MAPPS is used to tune the process flowsheet parameters to fit typical processing conditions. The flowsheet is then optimized a second time to determine processing conditions which optimize certain pulp properties while constraining yields. Results are discussed for a typical mechanical pulping flowsheet showing the development of properties and the influence of process steps on fiber flows and performance attributes.

Future work includes the extension of this approach to other pulping systems and to papermaking. We are also developing methods of incorporating an expert system capability into MAPPS to enhance the data handling and product quality predictions.

INTRODUCTION

Process simulation is now a widely used technique to compute heat and material balances in complex flowsheets. A number of process simulators are now used throughout the pulp and paper industry. These include sequential modular simulators such as GEMS and MAPPS and simultaneous simulators such as MASSBAL. Most simulators provide a wide range of process models for simulation of pulp mills, paper machines, bleach plants and steam and power systems. Simulators predict the flows of energy and mass or chemical components throughout the flowsheet. Economic evaluations over the flowsheet are now an important factor in corporate decisionmaking.

In addition to the simulation of these conventional and very important flows, knowledge of product quality, performance and properties is perhaps of even greater importance. Simulators generally lack the capabilities to predict product quality because of the causes of quality variations are not well understood or often depend on fundamental properties which are not conserved as are mass and energy. On the other hand, a great deal of quantitative as well as heuristic knowledge of the effects of fundamental variables and processing conditions on pulp properties has been developed at the Institute and elsewhere.

OBJECTIVES AND SCOPE

The MAPPS group at the Institute has sought ways to incorporate this knowledge into its process simulator to predict paper properties and process performance. Initially the scope of the development was limited to property development in mechanical pulping systems. It is possible to relate some product properties to a small group of relatively fundamental or intermediate properties of the fibers which can in turn can be determined throughout the process.

This paper describes the application of existing literature models and techniques to simulate pulp and paper properties using the MAPPS (Modular Analysis of Pulp and Paper Systems) developed at the Institute of Paper Chemistry. Applications of MAPPS to a variety of pulp and paper processing systems have been described previously by Parker (1,2) and Jones (3,4).

DISCUSSION

Four mechanical pulping modules were developed which simulate the main features of mechanical pulping processes. The modules simulate refining of chips and fibers, mixing and storage of fibers, separations by pressure screens, cleaning and shive removal, thickening and consistency control and hydrogen peroxide bleaching. Chemical and thermal pretreatment are accounted for indirectly through the process flag list described later.

Several mechanical pulping process flowsheets were developed and evaluated. A typical flowsheet, shown in Figure 1, includes a chip and secondary refiner, a reject refiner, primary

screen, two sets of cleaners, a bleaching stage, stock tanks and thickeners and deckers for consistency control.

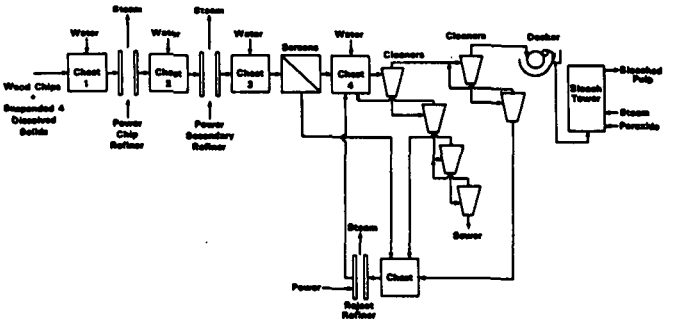

Fig. 1. High-yield pulping process.

Performance Attributes

The key aspect of the mechanical pulping modules is their use of performance attributes or PATs in the simulation. Each stream in Figure 1 now consists of the conventional stream data such as thermodynamic data and component flows plus a performance attribute substream containing PAT data as shown in Table I.

Table I. Mechanical pulping. Stream structures.

Physical Stream	Performance Attribute Substream
Number	Number
Type	Type
Temp.	Kappa no.
Pressure	Weight-average length
--	σ_L
--	Number-average width
Enthalpy	σ_w
Exergy	K-factor
Total flow	Canadian Standard Freeness
Component flows:	
Water	Absorption coefficient
Dissolved solids	Curl factor (latency)
Suspended solids	Fiber density
Chips	
Fiber 1	Fiber tensile strength
2	Fiber modulus
3	Cell wall thickness
4	
5	Process flag vector
Fines	
Shive 1	
2	
3	
H_2O_2	
H^+	
OH^-	
Dissolved lignin	
Na^+	
Inerts	

The stream variables are self-explanatory. The first 2 PATs identify the physical stream and the PAT type. The type defines the list of performance attributes of interest. The third parameter is a yield value such as the kappa number. Parameters 4 through 7 are the weight-average fiber length and standard deviation and the number-average fiber width and standard deviation. These parameters in addition to the fiber flows determine the detailed fiber length and width distributions at each point in the process. Parameter 8 is a surface-area development parameter defined originally by Strand and Edwards (5).

Parameter 9 is Canadian Standard Freeness, a commonly measured and controversial variable which correlates with most handsheet properties and relates to drainage rates. Parameter 10 is the light absorption coefficient which is reduced during bleaching. Parameter 11 is a latency parameter which relates to the development of latent pulp properties or to curl setting in the fiber during stock storage.

Parameters 12 through 15, average fiber density, intrinsic strength (zero-span tensile), modulus, and cell-wall thickness, affect the intrinsic strength and conformability of the fiber network. Parameter 16 is the process flag list, a sequence of numbers which qualitatively relates to the pretreatment conditions and process history.

The PAT structure is flexible and may be easily modified. Other, somewhat different PAT structures containing different sets of primary variables are under development for use in paper making, kraft pulping, recovery, and various bleaching sequences.

Quality and Performance Models

Property prediction depends on three types of models in MAPPS: process models, performance attribute models and property models as shown in Figure 2. Process models (Modules) compute mass and energy balances and determine fiber distributions. PAT models utilize information from process models and from entering PAT substreams to compute outlet PAT values. Property (quality and performance) models use process model and PAT parameters to compute property values. The property models used for high-yield pulps are based on the work of V. Venkatesh (6).

A performance attribute substream is created by MAPPS for each physical stream in the flowsheet. The appropriate process models have within them PAT models which modify the performance attributes. The PAT's are then passed on to the next module in the flowsheet just as the

physical stream data are passed. In the appropriate modules, information from the physical streams and the PAT's are combined and passed to the pulp and paper property models which print out properties at that point in the process.

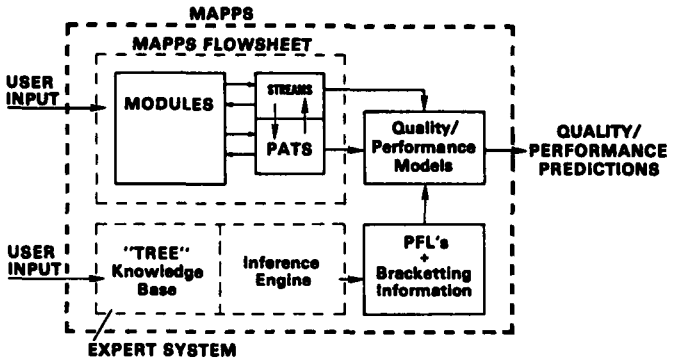

Fig. 2. Overview of quality and performance calculations with MAPPS.

Chip and Fiber Refining

The chip and fiber refiner modules are based on statistical and kinetic work of Yan, Corson, Irani and Epstein (7,8,9,10). The fiber size distribution of the inlet stream is changed by application of specific power to the refiner. Longer and wider fibers are converted to shorter and narrower fibers as shown in Figures 3 and 4 for a range of specific power. The chip refiner converts chips with a given average length and width into an outlet fiber stream containing a range of smaller fibers, shives and fines. The fiber refiner converts an inlet fiber stream into an outlet fiber stream.

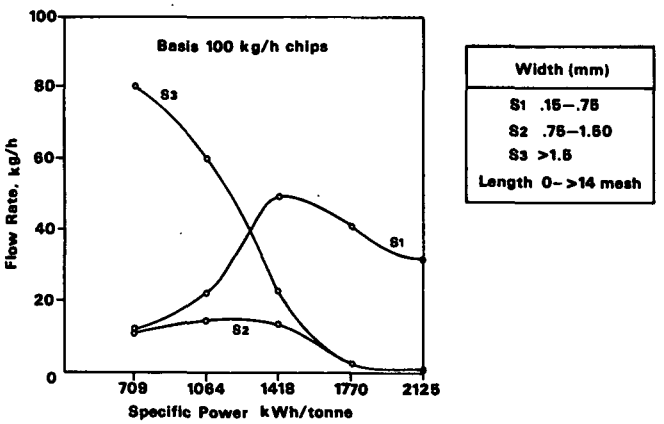

Fig. 3. Shive distribution from chip refiner at increasing specific power.

In addition to specific power are several adjustable parameters which represent the effect of design features on fiber size distributions.

Figures 3 and 4 show the variation in fiber distribution for increasing refiner specific power for a hypothetical chip refiner with chips averaging 25 mm in length and 5 mm in width being introduced.

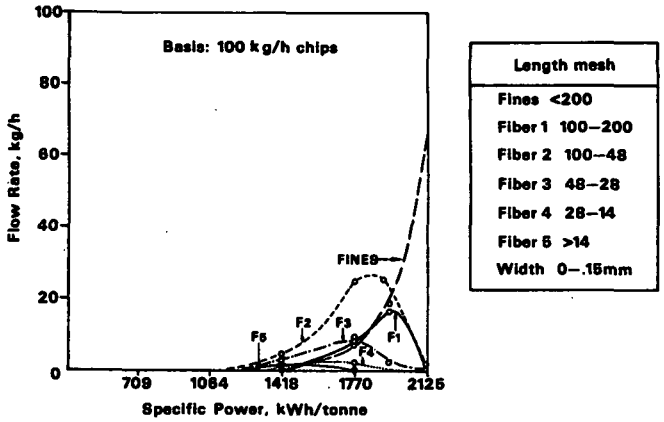

Fig. 4. Fiber distribution from chip refiner at increasing specific power.

Figure 5 shows the variation in weight-average length and width and number-average width over the same range of specific power. At low power most fibers produced are shives, while at high specific power most fibers are converted to fines. The preferred power is in the range of 1773 kwh/t where fines (less than 200 mesh), long fiber (fibers 4 and 5) and other fibers (1 through 3) are of roughly equal weight. The distribution parameters calculated by the module are placed in the PATs substream to be passed to another module. The models and techniques used will be described elsewhere (4).

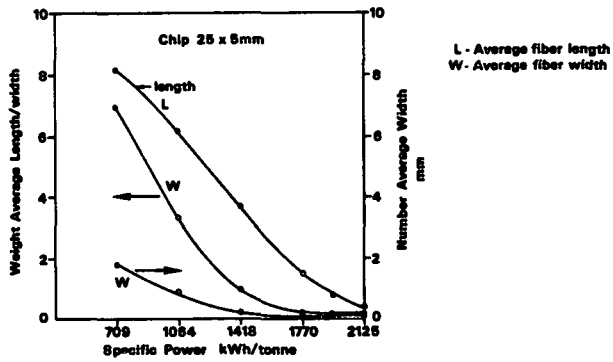

Fig. 5. Average length and average width of fiber from chip refiner at increasing specific power.

In each case both the average length and width decrease and the distributions become narrower. Lumped fiber components as shown in Table I are based on Bauer-McNett screen and Somerville slot width measurements. In general there is a rough positive correlation between length and width. The lumped component representation is not entirely useful in determining detailed fiber length and width distributions during refining.

The refining models, screening and cleaning and mixing models use a matrix representation

with 10 length ranges and 10 width ranges and 100 individual fiber lengths and widths. The upper limit on the largest length and width ranges is not fixed but depends on the average length and width and the shape of the distributions. The correspondence between the internal matrix representation and the lumped stream components is shown in Figure 6. This correspondence can be easily modified by the user to suit his application. DL and DW represent the weight-based length and width distribution density functions.

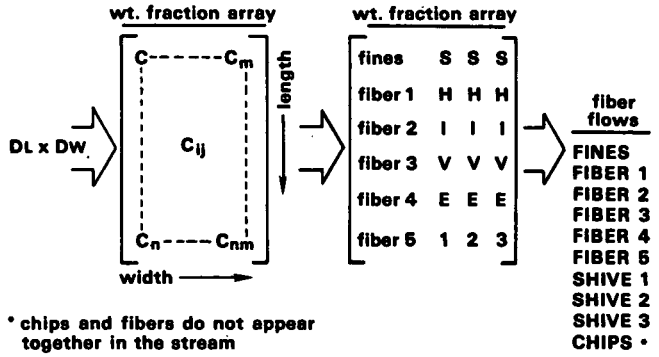

Fig. 6. Mapping of 100 internal fiber types to 9 fiber stream components.

Energy input for refining raises the temperature of the system. The result is steam formation and an increase in fiber consistency across the refiner.

Another PAT which changes during refining is the fiber specific surface area. The model of Strand and Edwards (5) is used to predict the specific surface area parameter, K-factor, from the consistency and the specific power input. The specific surface is computed from a second model which includes the K-factor and the fiber length distribution. There are separate models for both the primary and secondary refiner. The K-factor is carried in the performance attribute substream to compute specific surface where it is needed.

The Canadian Standard Freeness is another PAT computed by the refiner. Freeness is related to the surface area development of the fibers, i.e., to the formation of fibrils. The relation used is based on work by Stationwala and Atack (11), who found that natural log freeness is a linear function of hydrodynamic specific surface area and is relatively independent of plate design and wear pattern.

Fiber Mixing

Mixing of material and energy streams is normally a straightforward calculation. However, in the present application, we must mix performance attributes as well as materials. The difficulty is that many of the PATs are not conserved quantities. Fortunately, fiber dimensions and surface area are conserved during mixing and splitting operations which makes it possible to mix some PATs based on conservation of specific surface.

Weight average fiber dimensions are determined by computing the length and width distributions based on the weighted average of the length and width distributions of the entering streams. The technique used is described elsewhere (4). Mixing preserves specific surface area. Since freeness depends on K-factor which relates to specific surface, a conserved quantity, it is also possible to compute the mixture freeness.

All other mixture PATs, e.g., absorption coefficient, are equal to the weighted average of the inlet values. Mixing of PAT's in this fashion enables the mixture properties of different species and processing history to be determined. Table II shows the effects of mixing two streams on the mixture PATs and simulated properties. This particular mixture is unusual in that the high freeness screen rejects tend to dominate the properties of the mixture.

Removal of residual stresses and development of latent pulp properties is another poorly understood function of stock storage. This feature is discussed in a later section.

Fiber Screening and Cleaning

The principles of fiber separation are complex and highly dependent on geometrical factors and fiber properties. Detailed accounting of fiber length and width distributions offers an advantage over less detailed models of the fibers in predicting separation efficiency. By introducing PATs it is possible to develop more powerful models of fiber separation processes.

Two types of fiber separations considered are screening and centricleaning. In screening, separation occurs primarily based on fiber length or width (for slotted screens). Centricleaners separate by a combination of specific gravity and specific surface area. Specific surface area is also related to fiber length and width.

In the model used, the probability of rejecting a fiber depends on the total flow split (reject/total) and the length and width of each fiber. The mass flow of each fiber component in the accept and reject streams is

computed from the fiber separation efficiency and the fiber length and width distributions. The efficiency functions for the screen and centricleaner contain two adjustable parameters which represent details of the design and operation. The efficiency equations predict the reject split for each of the 100 combinations of fiber length and width used internally.

Table II. Simulation of fiber mixing on pulp and paper properties.

(TAPPI/CPPA except where noted)

	Screen Rejects	Second Cleaner Accept	Mixer to Second Cleaner Section
Fiber flow rate (kg/h)	45	25	70
PERFORMANCE ATTRIBUTES			
$\bar{L}$, mm	5.6	3.5	4.8
σ_L	1.8	9.0	4.7
$\bar{W}$, mm	0.049	0.025	0.027
σ_W	1.89	1.0	2.4
K-factor	0.207	0.207	0.207
CSF, mL	750	80	750
PROPERTIES			
Specific surface, m^2/g	1.0	7.9	--
Bulk, cm^3/g	5.1	7.75	5.0
Wet-web strength*, g	63.4	73	66
Tear index, $mN \cdot m^2/g$	15.7	6.1	15.7
Burst factor, $kPa \cdot m^2/g$	0	2.55	0
Breaking length, m	0	3400	0
Drainage time, sec	--	--	5.0
Specific light scattering coefficient*	--	--	400
Porosity, sec/100 cc	--	--	125
Opacity, %	--	--	90.7

-- Indicates no values available.

*SCAN method.

The performance attributes of the accept and reject streams are computed in the same fashion as for the mixer. Table III shows the separation of individual fiber components for a screen and the corresponding change in performance attributes for typical simulation conditions. The accept stream has a shorter average length and slightly smaller width, and a higher specific surface as measured indirectly by the lower freeness.

Table IV shows the corresponding change in properties with the accept stream containing a fiber with lower freeness, lower bulk, higher wet-web strength, higher tear index, lower burst index and higher breaking length than the inlet. The properties are reversed for the underflow stream.

Table III. Effect of separation processes on fiber size distributions.

Primary Screen

Total Flow Split 0.50 (reject/total flow)
Fiber Split 0.30 (accept/total fibers)

	Fiber Flow Rates		
	Entering	Accepts	Rejects
Fines	14.9	8.7	6.2
Fiber 1	6.6	2.4	4.2
2	16.3	5.0	11.3
3	7.5	1.4	5.1
4	3.0	0.5	2.5
5	7.9	1.2	6.7
Shives 1	12.6	1.3	11.3
2	0	0	0
3	0	0	0
Performance Attributes			
$\bar{L}$, mm	2.6	1.84	3.3
σ_L	4.9	4.82	5.6
$\bar{W}$, mm	0.069	0.068	0.07
σ_W	2.35	2.38	2.4
K-factor	0.245	0.245	0.246
CSF, mL	248	120	265

Table IV. Effect of separation processes on pulp and paper properties.

Primary Screen

TMP

Total Flow Split 0.50
Pulp Split 0.30

	Entering Fibers	Accept Fibers	Reject Fibers
Consistency, %	0.88	0.52	1.24
CSF, mL	247	121	265
Specific surface, m^2/g	5.3	6.7	4.3
Bulk, cm^3/g	3.5	3.0	3.7
Wet-web strength*, g	42	60	37
Tear index, $mN \cdot m^2/g$	15.2	16.3	13.6
Burst index, $kPa \cdot m^2/g$	0.8	1.0	1.4
Breaking length, m	2400	4400	2200

*SCAN method.

Tables V and VI show the effects of centricleaner separation on fiber distribution, performance attributes and handsheet properties. In addition to removing dirt and dense material, centricleaners also tend to segregate according to fiber aspect ratio. Only 10% of the narrow shives go to the accepts, while the overall pulp split is 52% accepts, for a total fiber split of 0.35 (i.e., 35% reject fibers/total fibers). For a 65% flow to the accepts, 52% of the fibers flow to the accepts. The average length in the accepts is greater, while the average width is smaller, i.e., the average length/width ratio is larger for the accepts. The freeness is also

higher for the accepts than the feed and is lower for the rejects. This is due to the higher fines content in the rejects. The K-factor does not appear to change much.

Table V. Effect of separation processes on fiber size distributions.

Primary Centricleaner

Total Flow Split 0.50 (reject/total flow)
Fiber Split 0.29 (accept/total fibers)

	Fiber Flow Rates		
	Entering	Accepts	Rejects
Fines	21	5.6	15.3
Fiber 1	5.9	1.7	4.2
2	11.6	3.4	8.2
3	3.0	1.2	1.8
4	0.7	0.4	0.3
5	1.4	0.8	0.6
Shives 1	2.0	0.2	1.8
2	0	0	0
3	0	0	0
	Performance Attributes		
$\bar{L}$, mm	1.3	1.4	1.2
σ_L	3.7	3.8	3.6
$\bar{W}$, mm	0.073	0.063	0.08
σ_W	2.5	2.4	2.61
K-factor	0.246	0.24	0.246
CSF, mL	132	150	118

Table VI. Effect of separation processes on pulp and paper properties.

Primary Centricleaner TMP

	Entering Fibers	Accept Fibers	Reject Fibers
Consistency, %	0.32	0.19	0.46
CSF, mL	132	150	118
Specific surface, m^2/g	6.5	6.0	6.8
Bulk, cm^3/g	3.0	2.9	3.0
Wet-web strength*, g	61.8	80.0	56.6
Tear index, $mN \cdot m^2/g$	17.6	16.6	18.3
Burst index, $kPa \cdot m^2/g$	0.7	0.5	0.9
Breaking length, m	4100	3300	4500

*SCAN method.

In Table VI, the specific surface of the simulated reject stream is somewhat higher than the inlet which reflects the lower freeness of the reject stream. The bulk and wet-web strength indicate a somewhat denser and stronger sheet from the accept stream, while the tear, burst and breaking length indicate more desirable characteristics for the reject stream.

Suspended material denser than water leaves with the rejects. Less dense and dissolved solids are split in the same proportion as water.

Consistency Control

Consistency is varied over a considerable range in the mechanical pulping flowsheet. Refining is usually done at a relatively high consistency from 30 to 50%, bleaching at 10 to 14%, screening at 1 to 2% and centricleaning at less than 1%. New medium consistency screening operations are now being introduced and could be easily simulated with these MAPPS modules.

Consistency is controlled to the desired levels in the flowsheet by use of gravity thickeners, slushers, and deckers. In this application it is assumed that no fibers enter the filtrate. The thickening process is approximated by splitting some water and dissolved components to the underflow to achieve the desired consistency in the overflow (accepts). The PATs of the accepts are the same as those of the inlet fiber stream. All PATs are zero in the reject water stream.

Yield Loss

Yield loss occurs in two ways: loss of fibers to the sewer from the cleaning system and lignin and shive reduction in bleaching. Any yield loss during pretreatment is currently assumed to be zero, although this can be taken into account through the use of an appropriate model to reduce the kappa number in the PAT substream.

Bleaching

Hydrogen peroxide bleaching is used in this application. Peroxide bleaches the fibers without significantly reducing lignin content. Chromophores in the lignin are oxidized by peroxide to insoluble carboxylic acids. These are neutralized in alkaline solution. Most color bodies change to a colorless form when oxidized. Color body removal reduces the absorption of light. The bleaching process is, therefore, measured by the reduction of the absorption coefficient with residence time.

The bleaching model is based on the extensive work of S. Moldenius (12,13,14). The overall rate depends on absorption coefficient (order is 2.2), peroxide concentration (order is 0.67) and alkalinity (order is 0.23). The rate constant has the usual Arrhenius dependence on temperature (activation energy = 45000 J/mole) but also a strong dependence on pulp consistency. This effect has not been explained in the literature and is unique to peroxide bleaching.

In addition to the consistency effect, the rate constant also depends on the initial pH of the solution. The apparent rate goes through a maximum with increasing initial pH. This is

explained by the competition between chromophore elimination and chromophore formation with elimination dominating except at very high pH. It is known that darkening occurs rapidly if the pulp is left at high pH.

Peroxide is consumed in proportion to the change in absorption coefficient. The relationship is linear with a slope which depends on both consistency and intial pH.

Acid is formed as the reaction proceeds. pH declines as the acids are neutralized in alkaline solution. This pH calculation is based on simplified acid-base equilibrium. It does not include the real system which contains sequestering agents, dissolved acids, salts, additives, etc.

The reactor is modeled as an adiabatic plug flow reactor. The bleaching rate is integrated along the length of the reactor to determine the values of Ck and reactant concentrations at each increment. The outlet absorption coefficient is placed in the PAT substream of the bleached pulp stream.

The module also calculates the following bleached pulp properties: sheet density, tensile strength, roughness, scott bond index, and tear strength based on Moldenius' data (14). Properties showed a significant cross correlation. Most of the properties were very similar in form to sheet density. Roughness showed an inverse response to density as expected.

Moldenius noted a significant improvement in properties with higher peroxide charge, a condition he referred to as hyperperoxide bleaching. Properties also increased significantly with increasing initial pH. The pH effect was larger at high peroxide charge. These factors are accounted for in the bleached pulp property models.

Bleached pulp properties were available for TMP, PGW and SGW processes.

DEVELOPMENT OF LATENT PULP PROPERTIES

Pulp fibers from the refiner contain residual stresses which cause the fibers to curl and become tangled into rolls, ribbons, and nodules. Fiber aggregates which are stored for significant periods above the wet lignin or wet hemicellulose softening temperatures and then cooled retain residual stresses. Hot disintegration allows the aggregates to untangle and the fibers to straighten. Under the right conditions, the fibers release their latent properties. After cooling, the fibers retain their latent properties. Cooling fibers while in contorted aggregates leads to latency being set into the fibers, i.e., inherent properties are lost. Latency removal depends on consistency, time, temperature, and shear history as well as the properties of the pulp itself and is therefore a rather complex kinetic process.

In the present models, it is assumed that latency has been removed. The properties reflect their full potential. However, a performance attribute to simulate latency, i.e., curl, has been provided. A model to relate stock storage conditions to curl and curl to fiber and paper properties must be developed before latency can be simulated.

Unbleached Pulp and Paper Properties

Frequently used pulp and paper properties are computed through the property interface and displayed as module parameters for the refiner, mixer, screen and cleaner units. Properties are adapted from correlations by Venkatesh (16). The models predict bulk, wet-web strength, tear factor, burst factor, breaking length, scattering coefficient, opacity and porosity based on TAPPI/CPPA or SCAN methods.

Performance Attribute and Property Development

Figures 7 and 8 show the variation and development in three performance attributes, weight-average length, number-average width, Canadian Standard Freeness and a related property, specific surface, throughout the flowsheet in Figure 1. Number-average width must be reduced to eliminate shives. Weight-average length is reduced as a consequence of refining, surface-area development and freeness reduction. Paper properties are increased by maintaining a relatively high long fiber content while increasing bonding area and reducing bending modulus.

Figures 8 and 9 also show the development of handsheet properties as the fiber attributes develop. Most handsheet properties improve as shives are eliminated. This is either a direct effect of shives or an indirect effect of surface area development. Some properties tend to improve as long fiber content is maintained, while other properties tend to improve as freeness is reduced.

Bulk declines or conversely sheet density increases steadily as shives are reduced and freeness decreased through refining. Similarly, drainage time steadily increases as freeness is reduced. Wet strength does not begin to increase until shives have been substantially eliminated, provided long fibers content is maintained relatively high. Breaking length gradually increases as shives are eliminated and freeness is reduced.

Tear and burst factors tend to decline as breaking length and tensile increase. Burst increases with decreasing freeness and with increasing levels of long fibers but also tends to be high when shives are relatively high. Tear factor decreases with decreasing freeness and may increase or decrease with increasing long fiber content, depending on the type of pretreatment. The sheet tends to become less porous as long fiber content increases. Porosity may increase or decrease with freeness depending on the type of pretreatment.

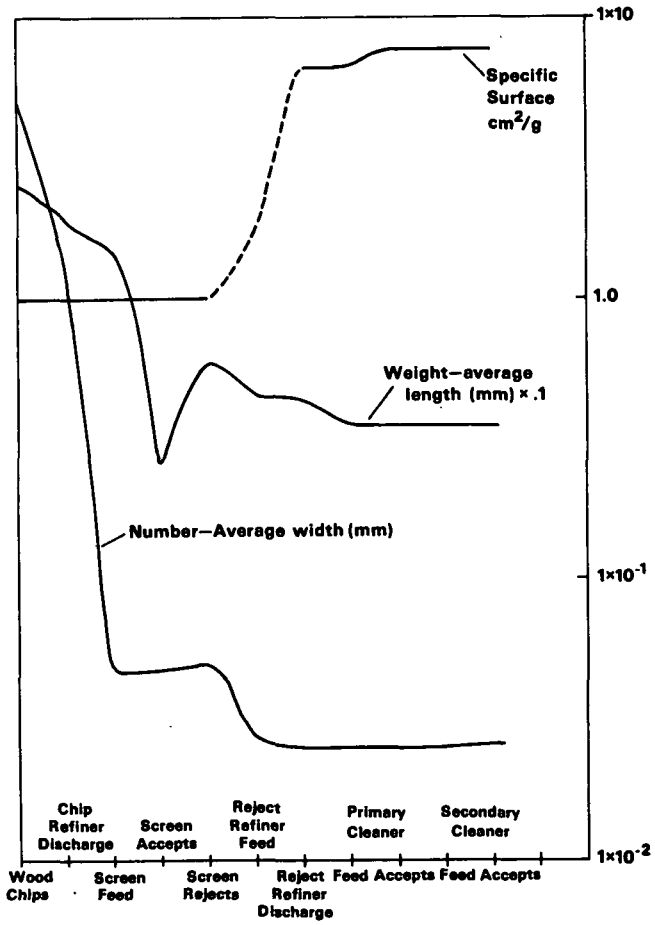

Fig. 7. Simulated performance attribute development.

Table VII shows the variation in lumped fiber component flows at the same points in the flowsheet. The basis is 100 kg/h of 25 x 5 mm chips. The yield on unbleached pulp is 99.35%. Only 0.65% of the fibers are lost to the sewer with the suspended solids. The differences between secondary cleaner accept flows and bleached pulp flows reflect a 2% lignin consumption and a 2% shive reduction during bleaching. Lignin consumed becomes dissolved lignin. The optimization process to be described in a later section has reduced shives content in the final product to 0.015% from a typical value of 0.1 to 0.4%. The bleached pulp has a relatively high long fiber content (36.2% greater than 28 Bauer-McNett mesh). Fines are relatively low at slightly over 18%. This results in a somewhat higher freeness of 85 compared to typical values of 30 to 50.

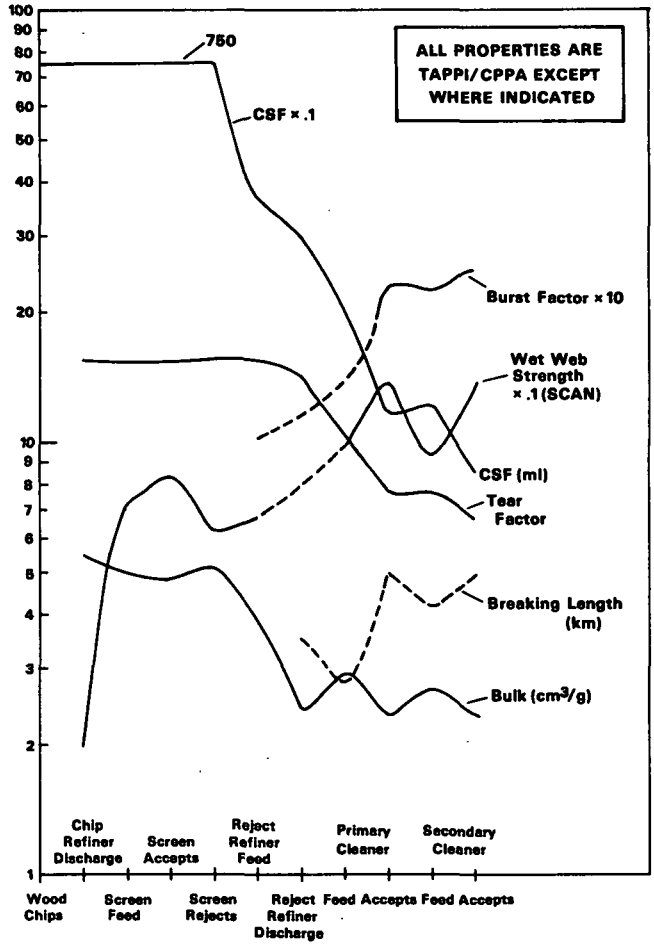

Fig. 8. Simulated property development.

Bleached Pulp Properties

Table VIII summarizes the overall changes occurring across the bleach tower. Entering are pulp and hydrogen peroxide in alkaline solution. The relevant performance attribute is the absorption coefficient, Ck, with an entering value of 8.0 m^2/kg. Pulp enters at 12% consistency. The alkaline peroxide stream enters at 316°K containing 4 to 6% peroxide by weight and a pH which varies from 11 to 12.2. Peroxide concentration varies between 0.12 to 0.16 moles/L. The tower residence time is varied by varying the tower volume which is scaled downward appropriate to the pulp flow. Stoichiometric coefficients and other model parameters are assumed constant. The effective reaction temperature is 311°K, the cup mixed stream temperature. The reaction consistency is 10.4%. Note that reaction time may be less than or equal to tower residence

time because the reactions may cease due to limiting conditions such as low pH or insufficient peroxide.

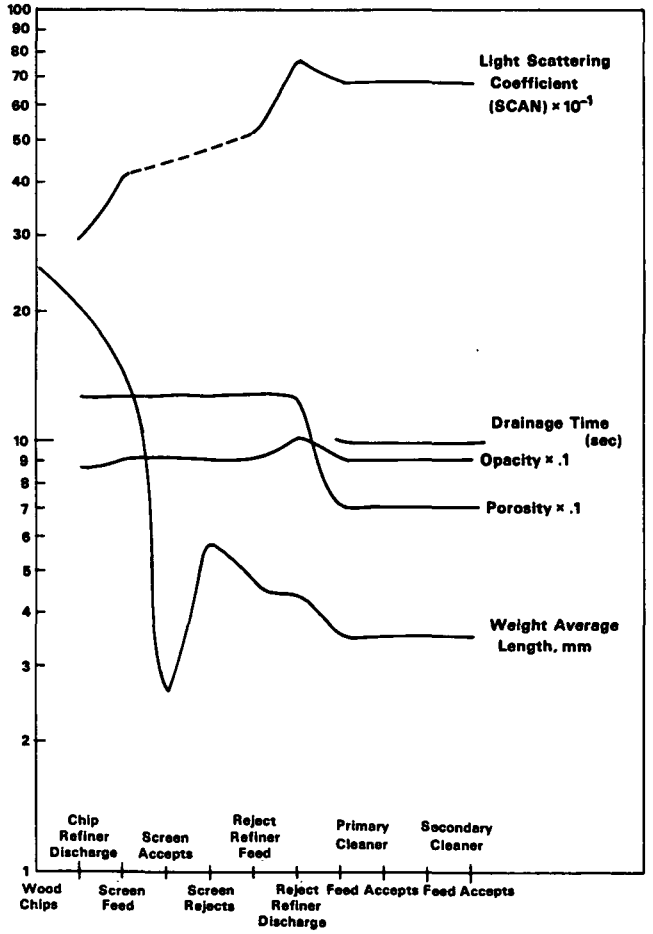

Fig. 9. Simulated property development.

For a 1 hour residence time, Ck drops to 3.77, the pH drops to 11.18 and 64% of the peroxide is consumed. Increasing residence time leads to a smaller additional reduction in Ck to 3.23 and a large reduction in outlet pH to 4.78. Properties are not affected by the additional bleaching.

When initial pH is dropped to 11, for a 3 hour residence time, the reaction effectively stops at a relatively high Ck of 7.53 due to the drop in pH to 3.5. Very little peroxide is consumed (7.1%). Properties deteriorate markedly. Tensile index drops from 35.5 to 26.7 and density (kg/m^3) drops from 0.454 to 0.380.

When the inlet pH is increased to 12.2, the reaction continues to 3 hours without a significant drop in pH. Outlet Ck is 2.99 and outlet pH is 11.3. Peroxide consumption is 76.4% by weight. Properties are only slightly improved. Inlet pH cannot be effectively increased much beyond 12.2 due to an increase in chromophore formation rate which counteracts the bleaching effect. Increasing the peroxide loading to 6% by weight or 0.18 g moles/L for a 3 hour residence time and inlet pH of 12.2 has essentially no effect.

In all cases the outlet fiber distribution and the quantity of dissolved lignin in the bleached pulp is constant.

Optimization

An optimization package containing two optimization routines, a successive linear programming (SLP) algorithm based on Griffith-Stewart (15) and a reduced gradient method (16, 17) is incorporated into the MAPPS package. Both methods may be used individually or successively. The SLP algorithm involves the repeated linearization and linear programming at each point in the search. In the reduced gradient method the variables are partitioned into two groups. A search direction is determined for one group, while the other group's values are changed during the search to maintain feasibility. A data file is used to define the independent and dependent variables and the initial guesses and bounds on the independent variables. A separate program defines the constraints and objective function in terms of combinations of independent and dependent variables.

A black-box approach is used. The flowsheet is converged at each iteration of the search. This convergence constrains the flowsheet to the feasible region. The dependent variables are passed back from MAPPS through the interface to the optimizer. A simple direct interface is used. The new independent variables are passed back to MAPPS from the optimizer through the interface. The process is repeated until no further minimization takes place.

The flowsheet was first optimized to fit typical unbleached pulp fiber distributions and freeness by adjusting the model parameters in each of the three refiners. The flowsheet was then optimized a second time by adjusting the specific power to each refiner and the flow splits over the screen and several of the cleaners to drive breaking length, tear, wet-web strength, burst and bulk to specified high or low values.

The optimizer increased the power to eliminate shives in the product and to maintain a high long fiber content. The freeness was also reduced further.

CONCLUSIONS

The capability of predicting handhseet properties of bleached and unbleached pulps is a step forward in process simulation. The introduction of performance attributes to provide a

Table VII. Simulation of fiber distributions.

TMP Process

Fiber Type	Bauer-McNett Class, (mesh)	Somerville Slot Width (mm)	Wood Chips	Chip Refiner Discharge	Component Flow Rates (kg/h) Screen Feed	Screen Accepts	Screen Rejects	Reject Refiner Feed	Reject Refiner Discharge	Primary Cleaner Feed	Primary Cleaner Accepts	Secondary Cleaner Feed	Secondary Cleaner Accepts	Bleached Pulp
Chips	--	--	100	0	0	0	0	0	0	0	0	0	0	0
Shive 3	All	W > 0.25	0	55.2	0	0	0	0	0	0	0	0	0	0
2	lengths	0.20 W < 0.25	0	32.3	0	0	0	0	0	0	0	0	0	0
1		0.15 W < 0.20	0	12.4	2.2	0.47	1.73	2.19	0	0.50	0.015	0.387	0.015	0.0145
Fiber 5	L > 14	W < 0.15	0	Trace	56.5	23.1	33.4	40.4	14.4	49.1	30.2	30.2	30.2	30.06
4	28 < L < 14	W < 0.15	0	Trace	7.2	4.0	3.2	4.6	3.4	9.7	6.0	6.0	6.0	5.96
3	48 < 1 < 28	W < 0.15	0	Trace	12.9	9.2	3.7	7.0	8.1	22.7	14.0	14.0	13.95	13.88
2	100 < L < 48	W < 0.15	0	Trace	14.7	12.5	2.2	7.9	16.5	38.0	23.4	23.4	23.4	23.04
1	200 < L < 100	W < 0.15	0	Trace	3.1	2.7	0.4	2.2	6.6	12.1	7.5	7.5	7.4	7.32
Fines	L < 200	W < 0.15	0	Trace	3.4	3.0	0.4	5.0	20.3	30.5	18.8	18.8	18.4	18.33
Dissolved solids		--	2	2	2	0.2	1.8	0.003	0.003	2.0	0	0	0	Dissolved lignin and other components not shown
Suspended solids		--	2	2	2	0.2	1.8	0	0	0.18	0.01	0.01	0.0	0
Consistency, %			30	50.5	1.01	0.61	4.5	30	57	0.13	0.09	0.09	0.09	10

Table VIII. Summary of bleaching case studies.

Temperature: 311°K
Consistency: 10.4%

Variables: Tower residence time 1, 2, 3 h
Inlet pH 12.1, 11, 12.2
Peroxide loading 0.12, 0.18 g mole/L

Case No.	Tower Residence Time (h)	Inlet pH	Peroxide Loading (g mole/L)	Reaction Time (h)	Outlet Absorption Coefficient (m^2/kg)	Outlet pH	Peroxide Consumption, (%)	Bleached Handsheet Properties Tensile Index (kNm/kg)	Scott Bond, (g/m^2)	Apparent Density (g/cc)	Bendtsen Roughness (mL/min)
1	1	12.12	0.12	1	3.77	11.2	64	35.5	104	0.45	757
2	2	12.12	0.12	2	3.23	4.8	73	35.5	104	0.45	757
3	3	12.12	0.12	3	3.21	4.8	73	35.5	104	0.45	757
4	3	11.0	0.12	0.11	7.53	3.5	7	26.7	93.5	0.38	196
5	3	12.2	0.12	3	2.99	11.3	76	35.7	141.8	0.46	758
6	3	12.2	0.18	3	3.0	11.3	76	35.7	141.8	0.46	758

link between the material flows and the properties is powerful and expandable to many types of processes other than the mechanical pulping discussed above.

The impact of process changes on product quality can now be analyzed.

Economic evaluation based on product and process performance as well as capacity factors will provide a more detailed picture, one more useful for decision-making.

FUTURE WORK

Future work must extend the PAT structure, and models to other pulping systems, particularly kraft and sulfite. High-yield bleaching by sodium hydrosulfite must be added. Development of more efficient and user-friendly ways of incorporating user data and information, particularly relating to properties and performance attributes, is another long range goal. In addition we are studying ways of combining expert system techniques with MAPPS existing structure to handle heuristic and qualitative information more effectively.

REFERENCES

1. PARKER, P. E. MAPPS-A Process Simulation Package for the Pulp and Paper Industry. Proceedings of the 11th IMACS World Congress on System Simulation and Scientific Computation, Oslo, Vol. 3 (1985).
2. PARKER, P. E. Process Simulation as a Decision-making Tool, PIMA, p. 34-39, (1986).
3. JONES, G. L. The Use of MAPPS in Academia. Supplementary Proceedings of the 1986 Eastern Simulation Conference, Norfolk, VA. 71, (1986).
4. JONES, G. L. Simulation of Product Quality and Process Performance. Proceedings of the 1987 Eastern Simulation Conference, Orlando, FL, (1987).
5. STRAND, B. D. AND EDWARDS, L. L. Tappi J. 67(12):72-75 (1984).
6. VENKATESH, V., Ph.D. Dissertation, U. of Idaho, (1976).
7. YAN, J. F. Kinetic Theory of Mechanical Pulping. Tappi J. 58(7):156-158 (1975).
8. CORSON, S. R. Size Analysis of Disc Re-

fined Pulp Distributions. Svensk Papperstid. (8):277-283 (1972).
9. IRANI, R. R. AND CALLIS, C. F. Particle Size: Measurement, Interpretation, and Application. New York, Wiley, 26-57, (1964).
10. EPSTEIN, B. Logarithmico-Normal Distribution in Breakage of Solids. I&EC 40(12): 2289-2291 (1944).
11. STATIONWALA, M. I. AND ATACK, D., International Mechanical Pulping Conference, Toronto, Canada, (1979).
12. MOLDENIUS, S. AND SJORGREN, B. J. of Wood Chemistry & Technol., 2(4):447-471 (1982).
13. MOLDENIUS, S. Svensk Papperstid. 85(15): R116-123 (1982).
14. MOLDENIUS, S., Ph.D. Dissertation, Swedish Royal Institute, (1983).
15. GRIFFITH, R. E. AND STEWART, T. A. Management Sci., 7(4):379-392 (1961).
16. WOLFE, P. Methods of Nonlinear Programming. In Recent Advances in Mathematical programming, ed., R. L. Graves and P. Wolfe, New York, McGraw-Hill, (1963).
17. ABADIE, J. AND CARPENTIER, J. Generalization of the Wolfe Reduced Gradient Method to the Case of Nonlinear Constraints. In Optimization, ed. by R. Fletcher, London, Academic Press, 49-64 (1969).